TRANSNAV
http://www.transnav.eu
the International Journal on Marine Navigation and Safety of Sea Transportation
Volume 19
Number 1
March 2025
DOI: 10.12716/1001.19.01.13

A Ship Weather Routing Optimization Method Incorporating Ship Seakeeping Model

Z. Han[1], Y. Zhou[2], J. Zhang[1] & D. Wu[1]
[1] *Wuhan University of Technology, Wuhan, China*
[2] *Beibu Gulf Port Co., Ltd., Nanning, China*

ABSTRACT: Weather routing problem represents one of the most significant advancements in ship energy conservation and emission reduction. Weather routing problems involve a numerous spatio-temporal ship motion states and weather characteristics, leading to challenges in consumption estimation and computational efficiency. To address this, an improved weather-state lattice-based method is first proposed, taking into account the ship's seakeeping model, weather characteristics, and consumption optimal control. The optimal energy conservation trajectory considering ship course under discrete motion states and weather characteristics is determined by optimal control and defined as motion primitives. Furthermore, the graph search method combined with the motion primitives is applied to generate the optimal energy trajectories. The results indicate that the framework can generate lower-consumption trajectories by leveraging weather-induced forces. Moreover, incorporating the seakeeping model into the weather routing framework not only enhances the accuracy of energy consumption estimation but also significantly improves the manoeuvrability of the generated trajectories.

1 INTRODUCTION

The reduction of energy consumption and greenhouse gas emissions has emerged as a critical focus in the sustainable development of marine transportation. Weather routing, a methodology that optimizes ship trajectories by harnessing weather-induced forces—such as wind, waves, and ocean currents—to minimize propulsion demand, has garnered considerable attention in maritime path planning research. Notably, ship energy consumption is affected by ship motion states, weather characteristics, which are both spatio-temporal variables. Thus, the development of an advanced weather routing framework, integrating weather effects on ship motion states is imperative for enhancing energy efficiency and operational sustainability.

Weather routing is commonly formulated as a path-planning problem under constant-velocity assumptions, typically addressed using graph-search methods such as the isochrone method [1], [2], A* algorithm [3], or probabilistic roadmap approach [4]. In these studies, energy consumption between adjacent nodes is estimated according to the ship constant velocity and weather conditions, and serving as directed edge weight for path searching. Furthermore, various studies introduce the time or velocity dimensions into grid map developments, while the improved path with velocity profile can be directly searched in 3D configuration space [5]. Meanwhile, to trade off various demands (navigation time, energy consumption, etc.) proposed by ship owner, numerous heuristic algorithms have been introduced and employed in this field, such as genetic [6] and ant colony algorithms [7]. Despite these methodological

advancements, several limitations persist due to simplifying assumptions in these studies. For instance, most existing methods neglect the ship manoeuvring model under varying weather conditions and only account for weather-induce forces in the surge direction, while disregarding their influence on sway and yaw. It leads to the resulting paths cannot be directly applied as reference trajectories, requiring additional smoothing to adapt to actual ship navigation.

To address this limitation, the weather-induced effects on ship motion have attracted significant attention, particularly their influence on other degrees of freedom. For instance, weather-induced lateral sway forces can significantly increase navigational drift, altering effective travel distance. Similarly, weather-induced yaw moments may restrict planned course alterations, compromising path feasibility. Traditionally, ship manoeuvring models primarily served controller design for path tracking, treating environmental forces as disturbances to be eliminated [8]. With advancements in wind, wave, and ocean current simulation, the influence of these weather characteristics on ship motion are further analysed and incorporated into ship manoeuvring model, referred to the seakeeping model [9]. Leveraging this model, the weather characters are considered as constraints, and the optimal control has been introduced to improve the trajectory performance [10]. However, these studies are typically applied in the static environment. In other words, the force and moments induced by weather characters are not a spatio-temporal variables, which is inconsistent with the transoceanic and long-term ship navigation.

To address this, the improved lattice-based path planning method considering discrete weather condition is proposed and utilized to plan the optimal trajectory. The motion primitives incorporate ship seakeeping model and discrete weather characteristics through optimal control, with energy consumption explicitly minimized in the objective function. Crucially, these motion primitives capture weather-induced force variations resulting from course alterations. The resulting navigation graph, constructed from these motion primitives, is then solved using graph search methods to determine the optimal path between origin and destination.

The paper is organized as follows: Section 2 details the proposed methodology. Section 3 presents numerical validation through comparative case studies. Conclusions are drawn in Section 4.

2 METHODOLOGY

Section 2.1 presents a 3-DOF ship seakeeping model that calculates weather-induced forces and moments acting on ship motion. This model serves as critical constraints for energy optimal control in Section 2.2. The energy-optimal motion primitives under discrete weather conditions are derived by optimal control and used in graph searching process to plan the minimum-energy trajectories in Section 2.3.

2.1 *3-DOF ship seakeeping manoeuvring model and energy optimal control*

The ship motion considering weather-induced force and moment is typically described by the 3-DOF seakeeping model as shown in Figure. 1. The ship's position and posture are typically described by the pose vector $\eta=[N,E,\psi]^T$ in North-East-Down (NED) coordinate system, where N and E denote the ship's position in the north and east directions, and ψ represents the yaw angle. The time derivative of the pose vector is determined by the velocity vector $v=[u,v,r]^T$ in body-fixed coordinates, where u, v, and r correspond to the surge, sway linear velocities, and yaw angular velocity, respectively and the rotation matrix J(leftψ), as expressed in Eq. (1) and Eq. (2):

$$\dot{\boldsymbol{\eta}} = \boldsymbol{J}(\psi)\boldsymbol{v}, \tag{1}$$

with

$$\boldsymbol{J}(\psi) = \begin{bmatrix} cos(\psi) & -sin(\psi) & 0 \\ sin(\psi) & cos(\psi) & 0 \\ 0 & 0 & 1 \end{bmatrix}. \tag{2}$$

The weather effects on the ship motion are formulated in the body-fixed coordinate. Generally, the irrotational ocean current is marked as v_{oc}, which combines with the ship's relative velocities v_r to determine the ships velocity over ground, as shown in Eq. (3). Furthermore, the wind-induced $\tau_{wind} = [f_u^{wind}, f_v^{wind}, f_r^{wind}]^T$, wave-induce $\tau_{wave} = [f_u^{wave}, f_v^{wave}, f_r^{wave}]^T$ and thrust force and rudder force moment $\tau = [f_u, f_v, f_r]^T$ determine the time derivative of relative velocity v_r, as indicated in Eq. (4),

$$\boldsymbol{v_r} = \boldsymbol{v} - \boldsymbol{v_c} \tag{3}$$

$$\boldsymbol{M}\dot{\boldsymbol{v}}_{\boldsymbol{r}} + \boldsymbol{C}(\boldsymbol{v_r})\boldsymbol{v_r} + \boldsymbol{D}(\boldsymbol{v_r})\boldsymbol{v_r} = \boldsymbol{\tau} + \boldsymbol{\tau_{wind}} + \boldsymbol{\tau_{wave}} \tag{4}$$

where, M includes both the rigid body and added mass terms, C represents the Coriolis-centripetal matrix, D is the hydrodynamic damping matrix, v_c signifies the ocean current velocity, which combines with the relative velocity vector to constitute the speed over ground.

The total ship resistance comprises the calm water resistance, wind resistance, and wave add resistance. While previous studies focus on the added force solely on surge direction, this study considers the weather-induced force and moments in 3-DOF (surge, sway, and yaw) direction. This comprehensive treatment captures the complete spectrum of environmental interactions affecting ship performance.

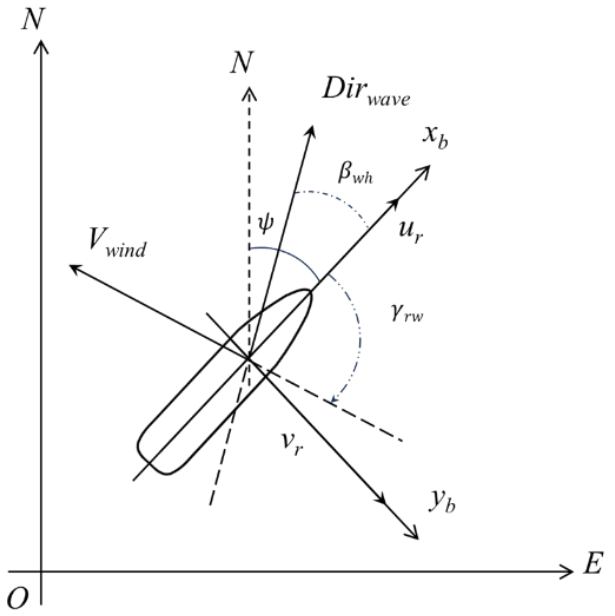

Figure 1. The seakeeping model in NED and body-fixed coordinates.

The ocean current force and moments is considered int hydrodynamic damping D matrix, as indicated in Eq. (5),

$$\boldsymbol{D}(\boldsymbol{v_r}) = \begin{pmatrix} X_{|u|u}|u_r| & 0 & 0 \\ 0 & Y_{|v|v}|v_r| + Y_{|r|v}|r| & Y_{|v|r}|v_r| + Y_{|r|r}|r| \\ 0 & N_{|v|v}|v_r| + N_{|r|v}|r| & N_{|v|v}|v_r| + N_{|r|r}|r| \end{pmatrix}, \tag{5}$$

where $X_{|u|u}$, $Y_{|v|v}$, $Y_{|r|v}$, $N_{|v|v}$ and $N_{|r|v}$ represent the hydrodynamic coefficients. The calm water resistance in the surge direction is determined by $X_{|u|u}$ in line with other weather routine research.

The wind force and moments acting on the ship seakeeping model are computed by ship velocity u and v, wind velocity V_w and angle of attack β_w, as shown in Eq. (6) and Eq. (7),

$$\begin{bmatrix} u_w = V_w \cos(\beta_w - \psi) \\ v_w = V_w \sin(\beta_w - \psi) \\ u_{ru} = u - u_w \\ v_{ru} = v - v_w \\ \gamma_{ru} = -\arctan(v_{ru}, u_{ru}) \\ \gamma_w = \psi - \beta_w - \pi \\ V_{ru} = \sqrt{u_{ru}^2 + v_{ru}^2} \end{bmatrix} \tag{6}$$

$$\boldsymbol{\tau_{wind}} = \frac{1}{2}\rho_a V_{ru}^2 \begin{bmatrix} C_x(\gamma_{ru}) A_{fw} \\ C_y(\gamma_{ru}) A_{lw} \\ C_n(\gamma_{ru}) A_{lw} L_{oa} \end{bmatrix} \tag{7}$$

where, u_{ru} and v_{ru} denote the surge and sway relative velocity, γ_{ru} denote the course between the ship velocity and wind velocity, ρ_a denote the air density, A_{fw} and A_{lw} represent the frontal and lateral projected areas, L_{oa} represent the length of ship, C_x, C_y and C_n represent the wind parameter depends on γ_{ru}.

The wave-induced forces and moments are functions of both the wave characteristics and the vessel's kinematic state. The sea state is modelled using the JONSWAP spectral density function $S(w|H_s,T_P)$, parameterized by significant wave height H_s, peak spectral period T_P, and mean wave direction β_{wave}, which accurately represents wave energy distribution for fully-developed open ocean conditions. The wave encounter frequency ω_e is derived by ship velocity V_s , wave frequency ω , the angle between the wave direction and the ship's course μ, while g represents the gravitational acceleration. in Eq. (8), thereby characterizing the effective wave energy spectrum acting on the ship.

$$\omega_e = \omega - \frac{\omega^2 V_s \cos\mu}{g} \tag{8}$$

The hydrodynamic response of a vessel to wave excitation is commonly characterized by the Response Amplitude Operator (RAO), denoted as C_{aw}. The wave energy density within a given frequency band can be derived from the wave spectrum $S_\zeta(\omega_e)$, adjusted for the encounter frequency ω_e , yielding the wave amplitude component ζ_0 according to Eq. (9):

$$\zeta_0 = \sqrt{2S_\zeta(\omega_e)\delta\omega_e} \tag{9}$$

Through spectral integration across all frequency components, the resultant mean wave-induced forces and moments are obtained as expressed in Eq. (10):

$$\bar{R}_{aw} = 2\int_0^\infty C_{aw} S_\zeta(\omega) d\omega \tag{10}$$

2.2 *Motion primitives determined by energy optimal control*

This section presents a quantitative evaluation of energy consumption for different path, and illustrates the application of optimal control to determine the most energy-efficient trajectory.

As illustrated in Figure 2, while all trajectories share identical origin, destination, and weather conditions, substantial energy consumption discrepancies emerge due to variations in initial and terminal course. Moreover, even with same origin and destination courses, course adjustments along the path generate different force profiles and corresponding energy consumption.

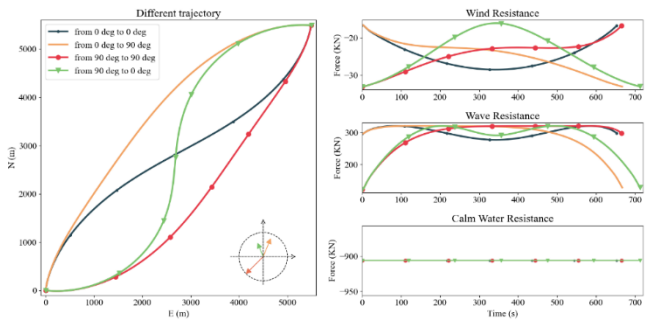

Figure 2. Weather-induced force in different trajectories.

Weather routing for energy conservation can be fundamentally formulated as an energy optimization

problem subject to weather-induced force and moment constraints. In the Section 2.1, the 3-DOF seakeeping model is introduced to describe the weather characteristic influence on ship motion, while is then transformed into equality constraints in the energy optimal control problem. The path planning algorithm enforces specified initial and end motion states as boundary conditions for trajectory optimization. Note that, the navigation time t_f is also regarded as the variable, which also be optimized by optimal control:

$$\{N(0),E(0),\psi(0),u(0),v(0),r(0)\}=\{N_{init},E_{init},\psi_{init},\overline{u_r},0,0\}, \tag{11}$$

$$\{N(t_f),E(t_f),\psi(t_f),u(t_f),v(t_f),r(t_f)\}=\{N_{end},E_{end},\psi_{end},\overline{u_r},0,0\}, \tag{12}$$

where N_{init}, E_{init}, ψ_{init}, N_{end}, E_{end}, and ψ_{end} represent the initial and end states, respectively, and $\overline{u_r}$ denotes the constant surge velocity under the chosen propulsion force.

In addition to this, the control inputs are bounds as Eq. (13) - Eq. (14),

$$f_{u_{min}} \le f_u(t) \le f_{u_{max}} \tag{13}$$

$$f_{r_{min}} \le f_r(t) \le f_{r_{max}} \tag{14}$$

In this problem, the optimization objective is the ship energy consumption, which is a combination of navigation time t_f, control input $\tau(t)$ and velocity $u_r(t)$.This study employs a constant relative velocity assumption, thereby reducing the objective function as shown in Eq. (15)

$$J(t)=\underset{x(t),\tau(t),t_f}{\arg\min}\, t_f\int_0^1 f_u(t)\,\mathrm{d}t, \tag{15}$$

$$\text{s.t.}\begin{cases}\text{Seakeeping maneuverability constraints Eq.(1) - Eq.(10),}\\ \text{Control input constraints Eq.(13) - Eq.(14),}\\ \text{Initial and terminal constraints Eq.(11) and Eq.(12).}\end{cases}$$

The optimal control problem, which necessitates consideration of the ship's motion state and weather conditions, presents a large configuration space that is challenging to solve directly. Thus, the optimal energy trajectory is derived under time-invariant environmental conditions. Moreover, the trajectory optimization problem for long-term navigation under spatio-temporal weather conditions is addressed through graph search method as shown in Section 2.3.

2.3 *State-lattice planner considering weather characteristic*

The graph search-based methods, such as the A* algorithm, serve as fundamental path planning techniques. Given the significant impact of weather-induced forces and moments on the ship sway and yaw DOF, the path between adjacent nodes is no longer regarded as a straight path. Consequently, the state lattice-based motion-planning approach, employed as a path search method accounting for ship seakeeping model and energy consumption optimal control, is integrated with weather condition in this study.

However, the computational burden of real-time optimal control between successive nodes remains prohibitive for practical applications in dynamic weather conditions. More critically, the combinatorial explosion of possible wind-wave-current interactions makes complete enumeration of energy-optimal solutions for all potential weather scenarios computationally intractable. the weather characters including ocean current velocity, wind velocity, wind angle of attack, significant wave height, wave period and wave direction are discretized. Directional parameters follow the standard 16-point compass division (22.5° resolution), maintaining compatibility with conventional navigational practices (north-east, north-west, etc). Weather condition intensity parameters are discretized according to the Beaufort scale and Douglas sea state classifications, as detailed in Tables 1 and 2, with threshold values adapted for regional conditions in the target navigation area. However, ship manoeuvrability becomes severely compromised under sea state code force 5 conditions, which generally exceed operational safety thresholds for commercial shipping. Consequently, this study explicitly excludes such hazardous conditions, treating all sea states beyond 5 as navigationally infeasible.

Table 1. Beaufort number table

Beaufort Number	Wind Description	Wind Speed (m/s)	Average Wind Speed (m/s)
0	Calm	0–0.51	0.255
1	Light Air	1.03–1.54	1.285
2	Light Breeze	2.06–3.60	2.83
3	Gentle Breeze	4.12–5.66	4.89
4	Moderate Breeze	6.17–8.23	7.20
5	Fresh Breeze	8.75–10.80	9.78
6	Strong Breeze	11.32–13.89	12.605
7	Near Gale	14.40–16.97	15.685
8	Gale	17.49–20.58	19.035
9	Strong Gale	21.09–24.69	22.89
10	Storm	25.20–28.80	27.00
11	Violent Storm	29.32–33.40	31.36
12	Hurricane-force	> 32.7	32.7

Table 2. Sea state code table

Sea State Code	Description	Wave Height (m)
0	Calm (like a mirror)	0
1	Calm (rippled)	0–0.1
2	Smooth (small wavelets)	0.1–0.5
3	Slight	0.5–1.25
4	Moderate	1.25–2.5
5	Rough	2.5–4.0
6	Very rough	4.0–6.0
7	High	6.0–9.0
8	Very high	9.0–14.0
9	Phenomenal	Over 14.

Furthermore, the ship's motion states require discretization to facilitate graph construction. As weather data typically exists in gridded format, the ship motion state N and E positional coordinates are discretized correspondingly. For comprehensive analysis of course-dependent energy expenditure, the yaw angle ψ is quantized in ψ increments. To maintain computational tractability, velocity states are simplified to a constant velocity $\overline{u_r}$, with zero lateral and rotational velocity components, thereby bounding the search space.

After determining the initial, end motion states and weather character combinations, the motion primitives consist of representative trajectories under various weather condition is obtained by optimal control as shown in Figure 3. The four circles in Figure 3 represent the level and direction of wave and ocean current. Note that, the trajectories with course information are

used to connect the adjacent nodes, which accounts for the ship's seakeeping model. Furthermore, due to weather difference, the minimum energy consumption trajectory derived from optimal control also varies. Compared with related approach that only considers the force in the ship surge direction, this method further improves the trajectory performance with the help of weather to affect the lateral force and torque of the ship.

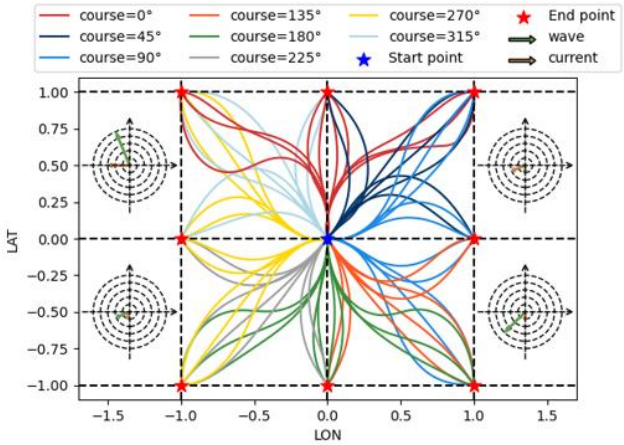

Figure 3. Motion primitives in different weather condition.

An example of the motion primitives with an initial course of 0 are presented, along with their fuel consumption and navigation time as shown in Figure 4. Due to the difference in weather conditions, the trajectories from the same initial state to the target position differ, and the trajectories are not symmetric. Both energy consumption and navigation time can be simultaneously reduced when navigating with favourable waves and currents. Therefore, a graph search algorithm must be employed to consider both the distance and energy-saving performance in order to generate the optimal path.

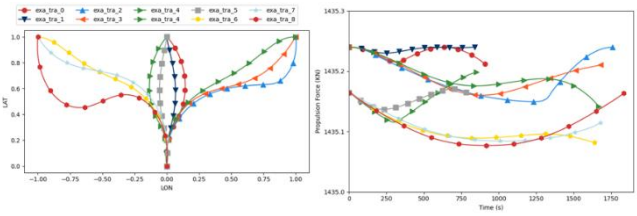

Figure 4. Propulsion difference in different weather conditions.

In line with A*, the cost function is divided into accumulated cost G and heuristic cost H. The path cost G is determined as the energy accumulation of multiple motion primitives, and the heuristic cost H is determined as the energy consumption estimation between nodes and destination without wind, wave and ocean current. It is noteworthy that, as the voyage duration to each node remains preserved, the varied weather conditions at individual nodes will undergo continuous temporal updates during the search process.

3 CASE STUDY

In this section, weather routine problem with different weather characteristics is analysed to evaluate the performance and efficiency of the algorithms. A container ship seakeeping model s175 with estimated RAOs in 3-DOF is used. To reduce the difficulty of the optimal control, only the quadratic terms of the ship's higher-order hydrodynamic effects in Damper matrix are retained. The estimated energy by this algorithm caused by course change is compared with other weather routing problems. Next, the advantage of the approach will be demonstrated caused by considering the seakeeping model. Lastly, the computational efficiency is assessed. All evaluations are conducted on a PC with an Intel i7 CPU@1.8GHz and 16GB of RAM.

In this study the proposed algorithm is validated in the North Atlantic within the longitude range of 74W to 5W and the latitude range of 45N to 55N. The weather data is obtained from ERA5 datasets with a time interval of 3h. Since the wind and current data in ERA5 have a resolution of 0.5° and the wave data has a resolution of 1°, all data will be interpolated to a uniform resolution of 1°. In this section, the great circle routing and conventional grid-based weather routing method A* is compared. The trajectories planned by three methods as shown in Figure 5, Figure 6 and Figure 7. In contrast to the influence of wind and current on energy consumption, wave impact exhibits a more substantial and immediate effect on ship power. Consequently, a comparative analysis is conducted between the shaft power output and wave-induced power, as shown in Figure 8– Figure 10.

The great circle route represents the shortest distance between the starting and destination points in the coordinate system, thus offering the minimum distance and shortest voyage time. However, as shown in Figure 6, the vessel's heading during 15 - 23 hours presents a bow-sea condition, resulting in significantly increased wave resistance. The vessel's shaft power approaches 10000 KW, exceeding the main engine's available power range. Furthermore, navigation under such sea conditions proves exceptionally challenging to maneuver, rendering this route unsafe.

Both the weather-conditioned A* algorithm and the weather state lattice approach generated navigational routes that strategically avoided regions with high wave conditions. Moreover, both algorithms optimized trajectories favoring following-sea navigation, leveraging wave action to provide additional propulsive energy and thereby reducing main engine power demand. While both conventional A* and weather state lattice algorithms produce paths with similar trajectory patterns, their energy consumption differs due to two primary factors. First, the A* algorithm employs fixed-path connections between adjacent nodes, whereas the state-lattice method dynamically adjusts vessel navigation between waypoints. Within each grid cell, it optimizes course variations to minimize wave resistance, as illustrated in Section 2.2 and Section 3.3. The second contributing factor stems from the seakeeping model's comprehensive approach. Rather than solely accounting for surge direction, it incorporates the lateral displacement effects induced by waves and

wind, thereby facilitating additional energy savings through optimized course corrections.

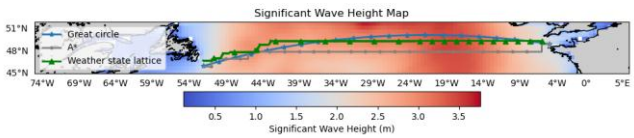

Figure 5. The trajectories planned by great circle, A* and proposed method in wave map.

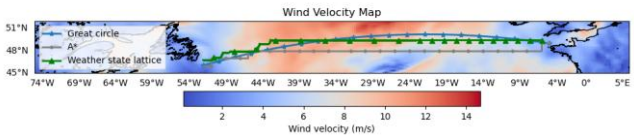

Figure 6. The trajectories planned by great circle, A* and proposed method in wind map.

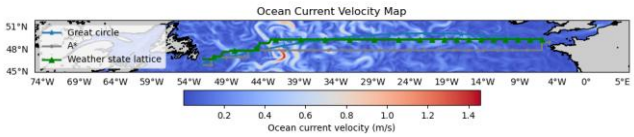

Figure 7. The trajectories planned by great circle, A* and proposed method in ocean current velocity map.

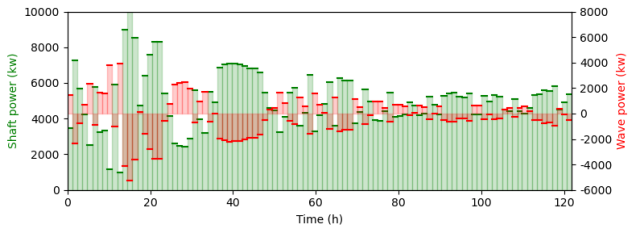

Figure 8. The shaft power and wave power along with the great circle routine.

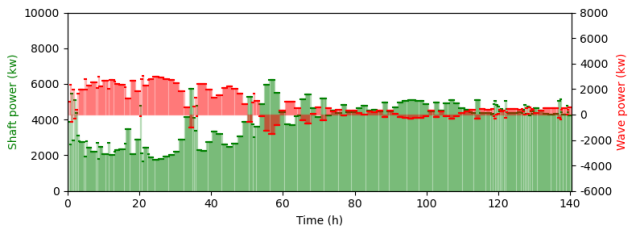

Figure 9. The shaft power and wave power along with the path planned by A*.

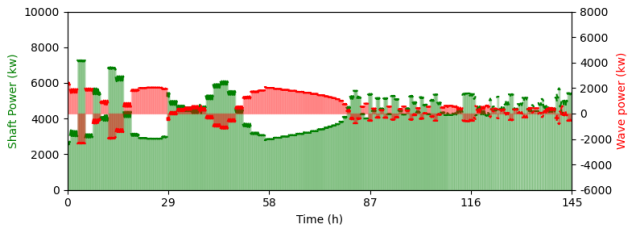

Figure 10. The shaft power and wave power along with the path planned by weather-state latticed.

Table 3. Trajectory method comparison.

Method	Navigation time (hour)	Energy consumption (kw*h)
Great Circle	121.89	577190.07
A* with weather condition	140.49	557656.45
State lattice	145.70	461831.49

Furthermore, conventional A* and great circle methods inherently lack vessel maneuverability constraints, frequently generating kinematically infeasible course alterations (e.g., abrupt 90° or 180° turns) that necessitate trajectory smoothing before being executable by the ship's control system. In contrast, our proposed state-lattice framework intrinsically incorporates the seakeeping dynamics, yielding navigation paths that are both optimized for energy efficiency and inherently compliant with the ship's maneuvering characteristics, thus requiring no additional preprocessing for execution.

4 CONCLUSIONS

This study presents an innovative method that integrates seakeeping model and optimal control for weather routine. The core of the methodology lies in a weather state-lattice approach that precomputes energy-optimal motion primitives across discretized environmental conditions while incorporating 3-DOF seakeeping model and optimal control. A graph search algorithm then connects these motion primitives, accounting for spatiotemporal weather transitions to enable global energy optimal between departure and destination. Validated through simulations in North Atlantic confirm the method's effectiveness in energy reduction and trajectory performance. The proposed method enables ship-specific weather routing optimization incorporating its seakeeping model.

REFERENCES

[1] Y. Chen and W. Mao, "An Isochrone-Based Predictive Optimization for Efficient Ship Voyage Planning and Execution," IEEE Trans. Intell. Transp. Syst., vol. 25, no. 11, pp. 18078–18092, Nov. 2024, doi: 10.1109/TITS.2024.3416349.

[2] H. Wang, X. Lang, and W. Mao, "Voyage optimization combining genetic algorithm and dynamic programming for fuel/emissions reduction," Transp. Res. Part Transp. Environ., vol. 90, p. 102670, Jan. 2021, doi: 10.1016/j.trd.2020.102670.

[3] Z. Song, J. Zhang, D. Wu, and W. Tian, "A novel path planning algorithm for ships in dynamic current environments," Ocean Eng., vol. 288, p. 116091, Nov. 2023, doi: 10.1016/j.oceaneng.2023.116091.

[4] N. Charalambopoulos, E. Xidias, and A. Nearchou, "Efficient ship weather routing using probabilistic roadmaps," Ocean Eng., vol. 273, p. 114031, Apr. 2023, doi: 10.1016/j.oceaneng.2023.114031.

[5] Y.-H. Lin, M.-C. Fang, and R. W. Yeung, "The optimization of ship weather-routing algorithm based on the composite influence of multi-dynamic elements," Appl. Ocean Res., vol. 43, pp. 184–194, Oct. 2013, doi: 10.1016/j.apor.2013.07.010.

[6] A. Kytariolou and N. Themelis, "Ship routing optimisation based on forecasted weather data and considering safety criteria," J. Navig., vol. 75, no. 6, pp. 1310–1331, Nov. 2022, doi: 10.1017/S0373463322000613.

[7] C. Zhang, D. Zhang, M. Zhang, J. Zhang, and W. Mao, "A three-dimensional ant colony algorithm for multi-objective ice routing of a ship in the Arctic area," Ocean Eng., vol. 266, p. 113241, Dec. 2022, doi: 10.1016/j.oceaneng.2022.113241.

[8] D. Mu, Z. Lang, Y. Fan, and Y. Zhao, "Time-varying encounter angle trajectory tracking control of unmanned surface vehicle based on wave modeling," ISA Trans., vol. 142, pp. 409–419, Nov. 2023, doi: 10.1016/j.isatra.2023.07.025.
[9] T. I. Fossen, "A NONLINEAR UNIFIED STATE-SPACE MODEL FOR SHIP MANEUVERING AND CONTROL IN A SEAWAY," Int. J. Bifurc. Chaos, vol. 15, no. 09, pp. 2717–2746, Sep. 2005, doi: 10.1142/S0218127405013691.
[10] N. Yang, D. Chang, M. Johnson-Roberson, and J. Sun, "Energy-Optimal Control for Autonomous Underwater Vehicles Using Economic Model Predictive Control," IEEE Trans. Control Syst. Technol., vol. 30, no. 6, pp. 2377–2390, Nov. 2022, doi: 10.1109/TCST.2022.3143366.